NRL/NUREG Report 8165

Significance of Warm Prestress to Crack Initiation During Thermal Shock

F. J. Loss, R. A. Gray, Jr., and J. R. Hawthorne

Engineering Materials Division

September 29, 1977

NAVAL RESEARCH LABORATORY
Washington, D.C.

Approved for public release; distribution unlimited.

20. (Continued)

In an experimental program, employing three-point bend specimens, it was demonstrated that warm prestress acts to elevate the "effective" K_{Ic} of the material at the crack tip. This elevation is not uniform; it depends on the WPS level, the degree of unloading, and the increment between the temperature of WPS and the failure temperature. However, WPS can result in an effective elevation in K_{Ic} to the WPS level, so that shallow cracks are arrested and deeper ones not extended. The experiments also demonstrated that failure never occurs during the unloading portion of the simulated LOCA path. Factoring WPS into an elastic analysis of crack extension during an LOCA results in predicted crack extension of greatly reduced proportions such that complete penetration of the wall does not occur.

The experiments show that the phenomenon of warm prestress should be considered in predictions of reactor vessel integrity, and that this phenomenon may form a key element upon which to base assurance of vessel integrity during an LOCA.

CONTENTS

BACKGROUND 1

APPROACH 2

EXPERIMENTAL INVESTIGATION 3

Material 3
Specimens 3
Experimental Apparatus 4
Loading Sequence 4

K_{Ic} TRENDS 6

WARM PRESTRESS TRENDS 7

ANALYSIS OF DATA 12

Experimental Trends 12
Theoretical Model 14
Effect of Biaxial Loading 16

STRUCTURAL INTERPRETATIONS OF WPS DURING A LOCA 16

SUMMARY AND CONCLUSIONS 20

ACKNOWLEDGMENTS 21

REFERENCES 21

SIGNIFICANCE OF WARM PRESTRESS TO CRACK INITIATION DURING THERMAL SHOCK

BACKGROUND

One of the postulated events for a nuclear pressure vessel is a sudden loss of coolant accident (LOCA)* followed by operation of the emergency core cooling system (ECCS). Introduction of the relatively cold ECCS water subjects the hot vessel wall to high thermal stresses, i.e., thermal shock. If the wall contains a cracklike defect at the inner surface, the stress intensity at the crack tip K_I increases with time to a maximum and then decays as the temperature gradient throughout the wall becomes smaller (Fig. 1). In addition, for highly irradiation-sensitive materials, neutron bombardment causes a marked shift to higher temperatures of the temperature dependence of the critical fracture toughness K_{Ic}. With a sufficiently high fluence level, the K_I and K_{Ic} curves can intersect, as illustrated in Fig. 1. At this point crack initiation would be predicted. Unfortunately, the magnitude of the ensuing crack extension cannot be easily computed, which has raised the possibility that cracks might penetrate the wall completely. However, decreasing fluence and increasing temperature toward the outside wall surface produce a steep gradient in toughness. This provides a mechanism for arrest of the running crack.

During the accident, the stress intensity for a flaw of given depth can attain the critical value for initiation within the first few minutes of the transient. Because the K_{Ic} level changes with time as a function of the changing temperature of the metal at the crack tip, the prediction of crack initiation does not necessarily correspond to the maximum K_I level. Under certain conditions, when the critical stress intensity is first achieved at a point where K_I is decreasing with time (see Fig. 1). The crack-tip material has been subjected to "warm prestress." In other words, the crack-tip region was subjected to a preload, at a higher temperature, that exceeded the K_{Ic} value at the lower temperature. Previous studies [1, 2, 3] suggest that warm prestress (*WPS*) elevates the "effective" fracture toughness of the crack tip so that crack extension will not occur when the stress intensity reaches the K_{Ic} value of the virgin material at the lower temperature. Another hypothesis is that, under LOCA conditions where K_I decreases with time, fracture cannot occur during the unloading because the decreasing strain at the crack tip eliminates a necessary condition for fracture. The preceding hypotheses for conditions associated with a LOCA must be verified in order to establish *WPS* as a meaningful basis for assuring vessel integrity.

Experimental studies with fracture mechanics specimens are being conducted at the Naval Research Laboratory (NRL) to characterize *WPS* under simulated LOCA loading conditions. This research will permit the qualification of the benefits of *WPS* during thermal

*A LOCA is defined as an instantaneous, double-ended break of a main coolant line to the reactor vessel. The vessel is assumed to be unpressurized for the entire accident analysis.

Manuscript submitted August 12, 1977.

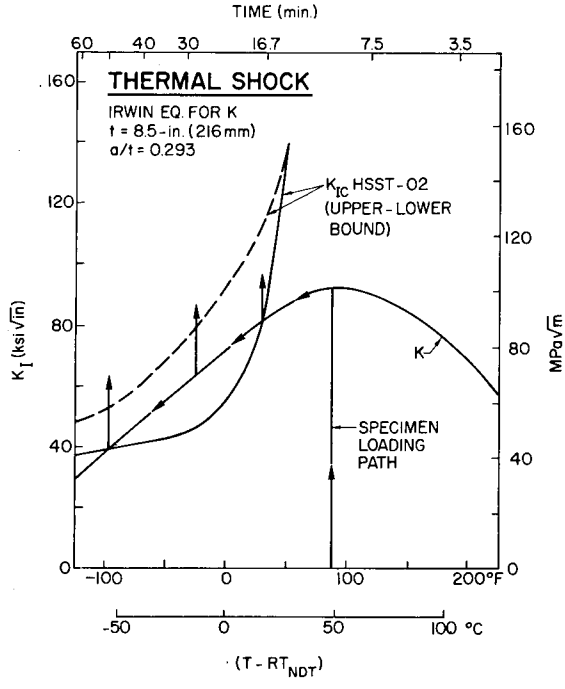

Fig. 1 — The K levels experienced by the material at the tip of a flaw in the nuclear pressure vessel undergoing thermal shock. The time scale originates with the LOCA; RT_{NDT} is the reference temperature as defined in Sec. III, ASME Boiler and Pressure Vessel Code.

shock and to better define the margin of safety against rupture of the vessel. An experimental program on thermal shock is also being conducted by Oak Ridge National Laboratory (ORNL) to evolve the capability of predicting the extension of preexisting flaws in small cylindrical sections of A508-2 steel subjected to a thermal shock [4]. It is anticipated that the NRL studies will provide an interpretation of the ORNL tests, and, in addition, to form a technical basis for projecting full-size vessel behavior in terms of *WPS*.

APPROACH

The objectives of the experimental phase of the NRL program were (a) to prove that *WPS* during a LOCA elevates the fracture toughness of the crack-tip region, and (b) to define the major parameters and their role in elevating the K_{Ic}. The most important objective was to translate the significance of a K_{Ic} elevation due to *WPS* into structural terms, showing how crack extension would be minimized in an actual vessel during a LOCA.

Investigation of the *WPS* phenomenon required an experimental simulation because loading an actual vessel is too costly. Small cylinders of the type tested by ORNL (53 cm, 21 in. OD), in combination with the existing ORNL thermal shock facility, are not adequate to simulate the *WPS* that occurs in a prototype nuclear vessel. Fortunately, it is believed

that the *WPS* effect encountered by the vessel can be simulated by mechanically loading three-point bend specimens that are notched and fatigue precracked. Therefore, experiments with bend specimens were conceived to maintain nearly plane strain conditions since this test conditions will also occur in a thick nuclear vessel. However, the unflawed vessel is subjected to thermally induced biaxial stresses (longitudinal and tangential) that are not precisely duplicated in the bend specimens.

The method of specimen loading was designed to achieve the following objectives:

(1) To limit the specimen crack-tip plastic zone to a size no larger than that which occurs in a thick vessel wall under plane strain constraint at the same applied K level.

(2) To fracture the specimens at a temperature low enough to ensure that the *WPS* level exceeds the K_{Ic} value of virgin material at the fracture temperature.

(3) To permit investigation of the relative importance of unloading path.

It is important to restrict the plastic zone size in the specimens (objective 1) so that any benefit attributed to the WPS phenomenon is not subject to the uncertainty that could arise if the simulated loading produced a plastic zone larger than that in a vessel wall during a LOCA. The specimens must be fractured at a temperature low enough that an elevation in the K_{Ic} caused by WPS can be detected unambiguously (objective 2). For example, consider a specimen loaded to failure at a temperature only slightly below the WPS temperature. At this temperature K_{Ic} may equal or exceed the WPS level K_{WPS}. If, as a consequence, the failure level K_F equals or exceeds K_{WPS}, the result might not be an elevation in K_{Ic}, but instead it could reflect the expected K_{Ic} behavior of the virgin material. Finally, it was felt that the shape of the unloading path could contribute to the WPS effect. The particular unloading path that occurs during thermal shock has not been previously investigated, and so it was necessary to consider the relative importance of variations in this parameter (objective 3).

EXPERIMENTAL INVESTIGATION

Material

The test specimens were fabricated from 300-mm (12 in.) thick A533-B1 steel plate obtained from the Heavy Section Steel Technology (HSST) program (HSST plate 02). This material was chosen because its static K_{Ic} trend as a function of temperature has been well characterized in thick sections [5,6]. Because the amount of HSST plate available was limited, electron beam welding was used to add end extensions to the test sections. During welding, the temperature of the test section was not significantly elevated because of the low and concentrated heat input of the electron beam.

Specimens

Specimens of two different thicknesses, 38 and 76 mm (1-1/2 and 3 in.), were prepared in the TL orientation. Because the test material was limited, the 38-mm specimens were machined from several thickness positions so that the midthickness for different specimens

ranged from the quarter thickness (1/4T) to 3/4T plate locations. The midthickness of all the 76-mm specimens corresponded to either the 1/4T or 3/4T position.

The three-point bend specimens were machined to ASTM E399 proportions with a span-to-width (S/W) ratio of 4.0. A portion of the specimens was face-grooved* in order to maintain a straight crack front representative of a long crack in a vessel. The specimens were fatigue precracked at a maximum K_I level of 27 MPa$\sqrt{\text{m}}$ (25 ksi$\sqrt{\text{in.}}$) to provide an overall crack depth-to-width ratio (a/W) of 0.42.

Experimental Apparatus

The specimens were loaded on a three-point bend fixture having roller supports at the outer edges. The fixture was surrounded by a cooling bath that was used to control the specimen temperature. The temperature was monitored by a thermocouple spot-welded to the specimen. Care was taken during cooling so that temperature differences throughout the specimen would be only a few degrees Celsius. Thus, any thermal stresses during cooling did not significantly influence the crack-tip K level as computed from the mechanical loading.

Two linear variable differential transformers (LVDT), one on either side of the specimen, were summed to monitor specimen deflections. Each LVDT was attached to the bend fixture and to the midspan loading roller. Because both the deflection of the fixture and the indentation by the rollers were small, the specimen deflections were measured directly by the LVDT.

Loading Sequence

The specimen loading sequence was designed to simulate a typical K_I vs temperature path of the crack-tip region as shown in Fig. 1. Warm prestressing was accomplished by slowly loading each specimen at room temperature to the desired K_{WPS} level. In all cases the level of fatigue precracking was significantly less than the K_{WPS} level. After loading to K_{WPS}, the load and temperature were decreased simultaneously along one of the paths illustrated in Fig. 2. Then, at a predetermined temperature, the specimen was isothermally loaded to failure. The temperature difference ΔT between the temperature of warm prestress T_{WPS} and the failure temperature T_F was chosen to represent that which could occur during a LOCA.

From an analysis of a reference calculational model (RCM) of the vessel [4], it can be concluded that the actual ΔT is a function of the relative crack depth a/W. For such a vessel, under worst-case conditions, the ΔT at the first intersection in Fig. 1 can vary, for example, from a minimum of 0°C at a relative crack depth of 0.2 to a value of approximately 95°C at a relative depth of 0.5. Hence, there exists no "typical" ΔT. In the present study, the ΔT values ranged from 100 to 220°C (Fig. 2). Although the smaller value more closely represents LOCA conditions, the larger values were chosen in order to investigate the importance of this parameter. Very small ΔT values (<25°C), which also represent LOCA

*The face grooves were machined to a depth of 5% of the thickness of each face. The grooves had a 45° included angle with 0.25-mm (0.010 in.) root radius.

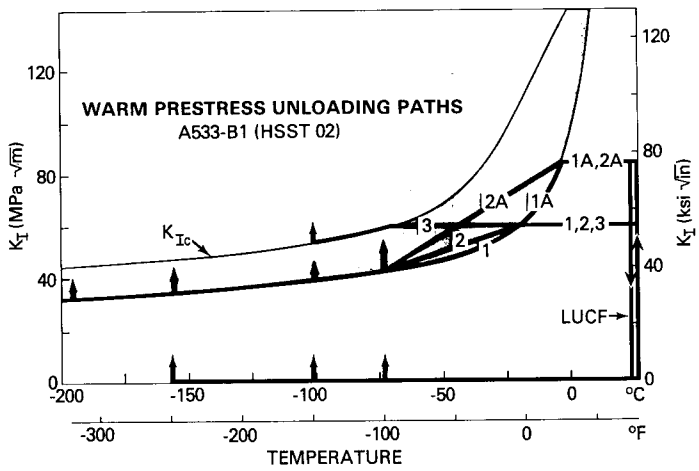

Fig. 2 — Unloading paths for warm prestress specimens. The vertical arrows, after the initial loading, designate isothermal loading to failure. The data for the K_{Ic} trend are given in Refs. 5 and 6.

conditions, were not used because the failure points would lie within the K_{Ic} data band for the material. In this event, assessment of the K_{Ic} elevation caused by *WPS* would require a statistical approach. This in turn would require more specimens than could be machined from the available material. Small ΔT values currently are being investigated at NRL in a follow-on program using a different heat of A533-B steel.

The specimen loading path in the subject study differs from that of a vessel material in two respects. First, the *WPS* was applied isothermally at room temperature, whereas the *WPS* in the vessel occurs with decreasing temperature. This difference should not change the resultant fracture behavior of the specimens vis-a-vis the vessel. For example, Andrews [3] has shown that a wide range of prestressing temperatures did not influence the fracture test results in *WPS* experiments. Second, the temperature increment ΔT in the experimental investigation was imposed at lower absolute temperatures than occur in the vessel. Since the program employs unirradiated material, the K_{Ic}-vs-temperature trend increases sharply at relatively low temperature (Fig. 3). Thus, an intersection between the K_I and K_{Ic} curves is possible only at temperatures lower than those which would occur in a vessel during a LOCA. In an irradiated vessel the intersection of the two curves occurs at higher absolute temperatures because irradiation causes a temperature shift of the K_{Ic} curve, by irradiation as previously described.

So that the specimen plastic zone would be restricted to a size no larger than that in a thick (plane strain) vessel wall at the same K level, the maximum K_I during *WPS* was limited to the plane strain measurement capability of the specimen as defined by ASTM E399, i.e., 59 MPa$\sqrt{m}$ (54 ksi$\sqrt{in.}$) for the 38-mm specimen and 84 MPa$\sqrt{m}$ (77 ksi$\sqrt{in.}$) for the 76-mm specimen. For a deep crack, however, the maximum computed K level for the RCM during a LOCA can exceed 200 MPa$\sqrt{m}$ [4]. For this reason some specimens were subjected to a K_{WPS} in excess of the ASTM E399 limit. Nevertheless, the specimen thicknesses and K_{WPS} levels used in the program are considered large enough to demonstrate and to quantify the *WPS* phenomenon.

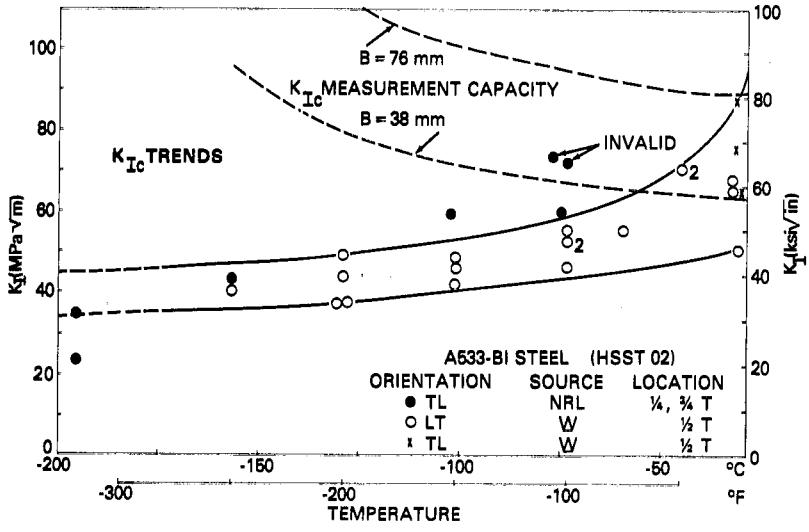

Fig. 3 — K_{Ic} trends for the program material [5,6]. NRL verification tests with 38 mm thick specimens suggest a somewhat larger scatterband. The K_{Ic} measurement capacity is defined by ASTM E-399.

K_{Ic} TRENDS

It is essential that the K_{Ic} trends for the test material be fully characterized so that the apparent elevation in K_{Ic}, attributable to *WPS*, can be assessed. The temperature dependence of K_{Ic} for the program material has been well defined by Westinghouse investigators [5,6]. A few additional verification tests were required because the specimens were not from exactly the same plate thickness position as the Westinghouse specimens. With respect to plate location, some of the NRL K_{Ic} and *WPS* specimens were machined from the broken halves of the Westinghouse K_{Ic} specimens. Other NRL K_{Ic} specimens were taken from a location adjacent to the plate section used for the Westinghouse tests. All of the Westinghouse specimens straddled the 1/2T plate. Due to the limited material, the NRL K_{Ic} specimens straddled the 1/4T and 3/4T planes. This sampling was considered acceptable because prior investigations of this plate [7,8] did not show a gradient in toughness through the thickness beyond a shallow (25 mm) layer at the surfaces.

Comparison of K_{Ic} data from both laboratories is presented in Fig. 3. Some of the NRL data unexpectedly fell outside of the Westinghouse data band. Although the scatter was not unreasonable, its cause has not been ascertained. The differences may be attributable to the different thickness positions used for the specimens from the two laboratories. The higher K_{Ic} values for the NRL specimens from the 1/4T and 3/4T locations, as opposed to the 1/2T location, would be consistent with higher toughness properties often observed at these locations in quenched-and-tempered materials. In analyzing the elevation of K_{Ic} by *WPS*, the "invalid" data in Fig. 3 were not considered.

WARM PRESTRESS TRENDS

Results from the 38-mm and 76-mm (1.5 and 3.0 in.) thick bend specimens are illustrated in Figs. 4 and 5, respectively, and are also listed in Tables 1 and 2. In both figures, specimens were loaded to a predetermined K_I level at room temperature (i.e., warm prestressed) and then simultaneously unloaded and cooled to the temperatures shown. This was followed by an isothermal loading to failure. The figures illustrate the behavior of two specimen loading patterns. The filled symbols denote a partial unloading (e.g., 30-60%) over the increment ΔT between the temperature of *WPS* (T_{WPS}) and the temperature of isothermal loading to failure T_F. The open symbols denote loading to K_{WPS}, unloading completely at T_{WPS}, cooling to T_F and failure by subsequent isothermal loading (LUCF). It must be emphasized that only the partial unloading path is representative of LOCA conditions; complete unloading to the point where K_I reaches the K_{Ic} level will not occur during the accident. The LUCF path, however, provided a means to characterize the significance of the degree of unloading.

For the interpretation of data trends, it is important to note first that no specimens failed during the simultaneous unloading and cooling, even though the critical K_{Ic} for the virgin material was attained. This behavior was expected in view of the decreasing strain at the crack tip associated with the unloading. This fact is of major importance to the vessel integrity as explained later. Next, note that with one exception discussed later, all specimens that were partially unloaded following the *WPS* exhibit a value of K_I at failure (K_F) exceeding the K_{Ic} value at the specific failure temperature. It is therefore concluded that *WPS* during a LOCA effectively elevates the K_{Ic} of the material at the crack tip. The specimens that were completely unloaded also exhibited an elevation of K_{Ic}, but to a lesser degree than those partially unloaded. In fact, no elevation in K_{Ic} was exhibited by specimens that were completely unloaded and then fractured at a very low temperature (-196°C, -320°F). Thus, the data suggest that the extent of the unloading (partial unloading vs complete unloading) does influence the specimen behavior. It appears, however, that the specific partial unloading path (paths 1, 2, 3, 1A, and 2A in Fig. 2) had no discernable influence on the results. This topic is considered in greater detail later.

The following observations were also made. First, the data exhibited no trend attributable to the face grooves. This was not unexpected because of the crack-front curvature of the fatigue precrack in both specimen types. A typical example of the precrack shape is shown in Fig. 6. The crack front of the face-grooved specimens was generally straight; the ungrooved specimens did exhibit precrack tunneling but this tunneling was not large. About one-half of the specimens in Figs. 4 and 5 were face grooved. Second, the linear nature of the load vs deflection records for the specimens suggested an absence of plastic bending and stable (ductile) crack extension during *WPS* and during the path leading to fracture. This deduction was confirmed by the fracture appearance of all specimens. As illustrated in Fig. 6, the crack extended from the fatigue precrack entirely in the cleavage (brittle) mode. The latter fracture mode is consistent with fractures representing plane strain behavior in this steel. Third, no firm conclusions regarding the benefits of *WPS* can be drawn from the group of data in Fig. 4 at -73°C for the lower prestress. Comparing these data with the NRL K_{Ic} data of Fig. 3 at the same temperature, shows that the K_F levels exceed only marginally the upper boundary of the K_{Ic} scatterband as it could be drawn to encompass the valid NRL K_{Ic} data. Consequently, the benefits of *WPS* under those conditions cannot be readily ascertained. This problem results from the choice of too small a ΔT (i.e., $T_{WPS} - T_F$), as discussed earlier. On the other hand, it should be noted that the values of K_F in this case

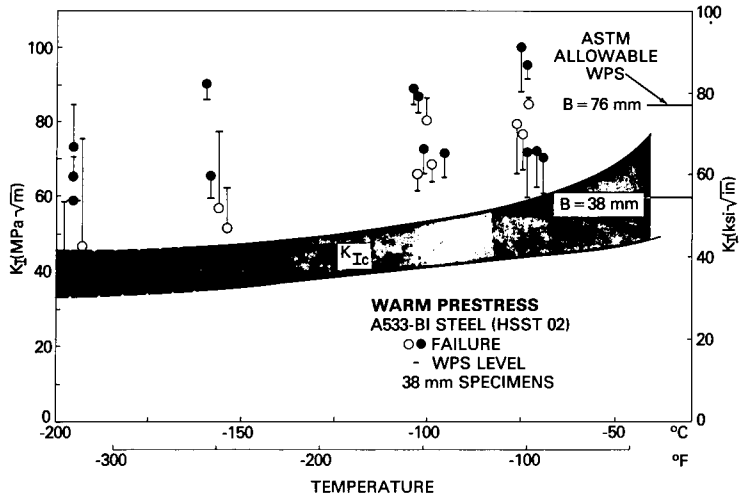

Fig. 4 — Warm prestress trends for 38-mm-thick specimens. The open circles represent the LUCF unloading path; the filled circles represent partial unloading paths illustrated in Fig. 2. The K_{Ic} band is taken from Fig. 3.

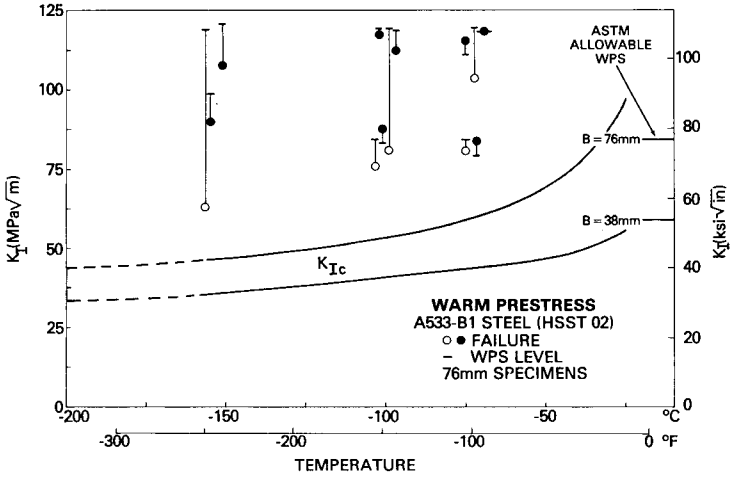

Fig. 5 — Warm prestress trends for the 76-mm-thick specimens. The open circles represent the LUCF unloading path; the filled circles represent partial unloading path 2A in Fig. 2.

consistently exceeded K_{WPS}. If there were no benefit from *WPS*, one would have expected some of the K_F values to be within the adjusted K_{Ic} band.

As illustrated in Figs. 4 and 5, the specimens were subjected to different levels of *WPS*. The lower level in each case corresponds to the ASTM E399 allowable for its specific thickness. In the case of the 38-mm specimen (Fig. 4) the higher *WPS* level corresponds to that

Table 1 — Warm Prestress Data for 38 mm Specimens

Spec. No.	FG*	*WPS***			Unloading Path†	Minima			Failure			K_F
		Temp (°C)	Load (kg)	K_{WPS} (MPa$\sqrt{m}$)		Temp (°C)	Load (kg)	K (MPA$\sqrt{m}$)	Temp (°C)	Load (kg)	K_F (MPa$\sqrt{m}$)	K_{WPS}
02 BU-7	X	16	7477	59.3	2††	-73	5272	41.8	-73	8909	70.8	1.19
BU-3	X	18	7463	62.1	1††	-73	5068	42.1	-73	8636	71.8	1.16
BU-4	X	21	8472	60.4	1††	-73	5727	40.7	-73	9804	69.9	1.16
BU-6	X	24	7488	67.6	LUCF	—	0	—	-73	8409	75.8	1.12
CA-8	X	24	8113	65.9	LUCF	—	0	—	-76	9659	78.5	1.19
BU-11		20	11568	91.5	2A	-73	5681	44.9	-73	11977	94.7	1.03
BU-12		85	11022	88.2	2A	-75	5636	41.2	-75	12409	99.3	1.13
BU-9			N/A		K_{Ic} Test		N/A		-76	7681	59.2	—
JV-10	X		N/A		K_{Ic} Test		N/A		-77	8204	73.7	—
BU-10			N/A		K_{Ic} Test		N/A		-73	8895	71.9	—
BU-8		21	7540	64.8	1	-96	4772	41.1	-96	8213	70.7	1.09
JV-6	X	20	7659	65.8	3	-112	5545	47.6	-101	8377	72.0	1.09
JV-7	X	20	7404	63.8	LUCF	—	0	—	-99	7845	67.7	1.06
CA-1		24	8136	61.2	LUCF	—	0	—	-101	8590	74.6	1.06
JV-1	X		N/A		K_{Ic} Test		N/A		-102	6431	59.6	—
CA-4		24	10931	84.7	1A	-104	5318	41.2	-104	11409	88.5	1.04
CA-9		24	10090	82.4	1A	-103	4977	49.7	-103	10568	86.4	1.05
CA-10		24	6954	59.2	1	-158	4977	42.4	-158	7590	64.6	1.09
CA-12		24	8022	62.3	LUCF	—	0	—	-154	6727	52.4	0.84
CA-3		27	10627	85.8	1A	-159	4659	37.6	-159	11090	89.6	1.04
CA-6			N/A		K_{Ic} Test		N/A		-157	5295	41.8	—
CA-11		24	7272	58.9	1	-196	3181	25.8	-196	7273	58.9	1.00
JV-3	X	21	8295	70.4	1	-196	2840	24.1	-196	7682	65.2	0.93
CA-2		24	10986	84.3	1A	-196	3545	24.4	-196	9431	72.9	0.86
CA-7			N/A		K_{Ic} Test		N/A		-196	3931	34.0	—
JV-2	X		N/A		K_{Ic} Test		N/A		-196	2909	23.6	—

*X designates face grooves
**Warm prestress
†Unloading paths are defined in Fig. 2
††*WPS* applied twice

Table 2 — Warm Prestress Data for 76 mm Specimens

Spec. No.	FG*	*WPS***			Unloading Path†	Minimums			Failure			K_F
		Temp (°C)	Load (kg)	K_{WPS} (MPa$\sqrt{m}$)		Temp (°C)	Load (kg)	K (MPa$\sqrt{m}$)	Temp (°C)	Load (kg)	K_F (MPa$\sqrt{m}$)	K_{WPS}
02 JU-3		18	40636	111.3	2A	-73	19681	54.0	-73	44181	115.5	1.04
JU-1		23	31045	84.6	LUCF	-73	0	0	-73	29681	80.9	0.96
JX-4	X	24	28000	79.4	2A	-73	14318	40.5	-73	29590	84.0	1.06
JX-2		24	43227	119.7	LUCF	-73	0	0	-73	37454	103.7	0.87
JV-2	X	24	41227	118.9	2A	-73	15272	44.1	-73	41227	118.9	1.00
JX-1		24	30181	83.4	2A	-101	14818	41.0	-101	31681	87.6	1.05
JW-4	X	24	41227	119.4	LUCF	-101	0	0	-101	27909	80.9	0.68
JX-3		24	30909	84.7	LUCF	-101	0	0	-101	27636	75.8	0.89
JV-1	X	24	40954	118.8	2A	-101	13681	40.0	-101	40682	117.9	0.99
JU-2		24	43363	118.9	2A	-101	14863	40.8	-101	41045	112.5	0.95
JW-2	X	24	41545	120.7	2A	-151	13818	40.2	-151	37090	107.8	0.89
JW-3	X	24	41318	119.1	LUCF	-157	0	0	-157	21818	63.0	0.53
JU-4		24	36136	96.3	2A	-157	12863	34.3	-157	32909	87.7	0.91

*X designates face grooves
**Warm prestress
†Unloading paths are defined in Fig. 2

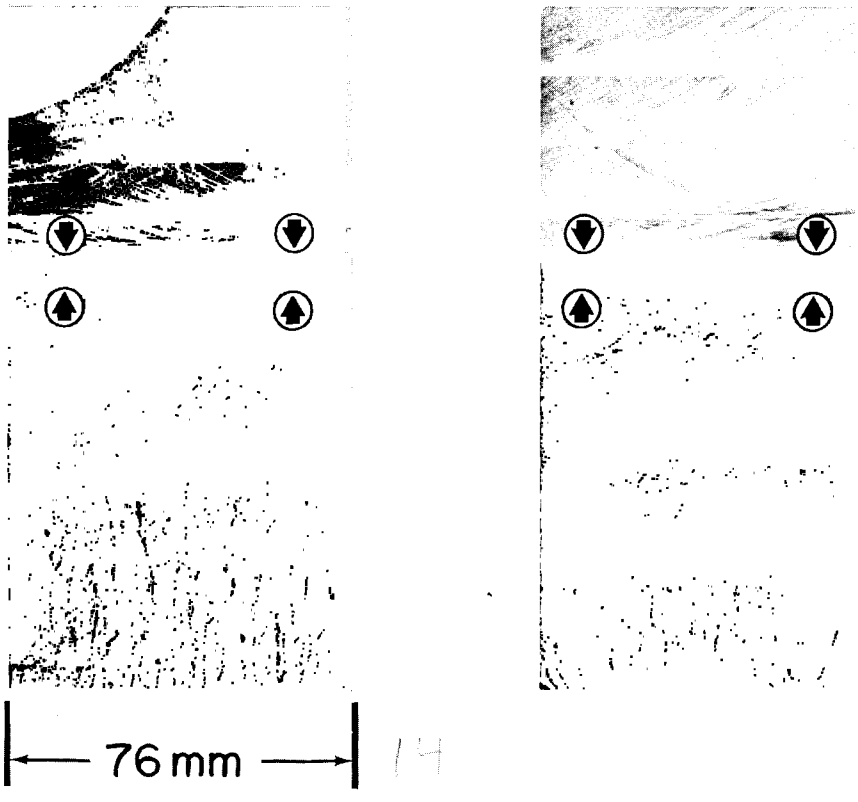

Fig. 6 — Typical fracture appearance of WPS specimens. Shown are fracture surfaces from 76-mm specimens with face grooves (right) and without face grooves (left). The arrows indicate the fatigue precrack. The mode of fracture is entirely cleavage (brittle).

permitted for a specimen of 76 mm or greater thickness. For the 76-mm specimens the higher *WPS* level corresponds to the allowable value for a 152 mm (6 in.) or greater thickness specimen. No differences are apparent between the trends in Fig. 4 for the 38-mm specimens prestressed to 80 MPa$\sqrt{m}$ (the ASTM allowable for a 76-mm specimen) and the trends in Fig. 5 for the 76-mm specimen prestressed to the same level. Also, the fracture surface appearance was similar for both specimen thicknesses. This correspondence suggests that the larger plastic zone resulting from the "overload" to 80 MPa$\sqrt{m}$ of the 38-mm specimens is not a deterrent factor in assessing the effects of *WPS*. On this basis, it is concluded that the geometrically similar overload of the 76-mm specimens to approximately 120 MPa$\sqrt{m}$ (Fig. 5) would also represent the behavior of 152-mm-thick specimens, had they been available for test. This conclusion is significant in that it permits a more general interpretation of the benefits of *WPS* to the higher *K* levels that may be experienced by a vessel during a LOCA.

ANALYSIS OF DATA

Experimental Trends

The magnitude of the K_{Ic} elevation by *WPS* can be observed from Figs. 4 and 5. It is not possible to assign a fixed value to this elevation in terms of, say, K_F/K_{Ic}, because K_F depends upon (a) *WPS* level, (b) failure temperature, and (c) degree of unloading. However, it should be noted that for a given failure temperature and unloading path, K_{Ic} is elevated in proportion to the magnitude of K_{WPS}. Thus, it appears that a high value of K_{Ic} could be obtained at a low temperature simply through the application of a high level of K_{WPS}.

The preceding is a simplistic analysis of the *WPS* phenomenon. More insight can be gained by considering the interaction of the three major independent parameters listed above and illustrated in Figs. 7 and 8. Figure 7 shows the *WPS* benefit in terms of the K_F/K_{WPS} ratio; the *WPS* benefit in terms of K_{Ic} elevation is more clearly shown in Fig. 8. From Fig. 7 it can be concluded that the maximum benefit of *WPS* is obtained for the case of partial unloading, small ΔT and low K_{WPS}. Fortunately, during a LOCA, two of the preceding three conditions are met. First, the metal at the crack tip is never completely unloaded—the unloading is not expected to exceed the 30 to 60% to which the specimens were subjected. Second, during a LOCA, the ΔT is expected to be small between the temperature of peak applied K_I and the temperature at which K_I attains the K_{Ic} level. A ΔT of 100°C, corresponding to a T_F of -73°C for the present studies, may represent the largest value that could occur. Consequently, the partial unloading data at -73°C in Fig. 7 would be most applicable to a LOCA. From this it can be concluded that for a K_{WPS} up to 120 MPa$\sqrt{\text{m}}$ (109 ksi$\sqrt{\text{in.}}$), the *WPS* phenomenon will (a) provide an effective elevation of K_{Ic}, and (b) assure that the failure level will equal or exceed the level of *WPS*. Furthermore, by extrapolating the partial unloading trend of Fig. 7 to higher values of T_F, it can be inferred that K_F/K_{WPS} may exceed unity at K_{WPS} levels even greater than 120 MPa$\sqrt{\text{m}}$. This conclusion would be associated with the smaller values of ΔT that could occur during a LOCA.

Figure 8 presents an alternate way to interpret the interaction of *WPS* level, failure temperature, and degree of unloading. This figure clearly shows that the elevation in K_{Ic}, as reflected by K_F, increases with the *WPS* level. The magnitude of the K_{Ic} elevation can be observed by comparing K_F with the mean K_{Ic} values for the appropriate failure temperature. For example, a K_{Ic} elevation in excess of 100% is exhibited by the extreme of the partial unloading data at -73°C; whereas, essentially no elevation in K_{Ic} is exhibited by the LUCF data at -196°C.

As with Fig. 7, an extrapolation of the trend illustrated in Fig. 8 suggests that even higher elevations in K_{Ic} could be obtained with the higher imposed values of K_{WPS}. However, one should also note the deviation from the one-to-one relationship between K_F and K_{WPS} as K_{WPS} is increased. The reason for this deviation is believed to be related to the interaction of (a) the compressive residual stresses that can cause reverse yielding upon unloading of the crack tip, and (b) the elevation of the yield stress due to temperature that results when a large ΔT is employed. This interaction is considered next.

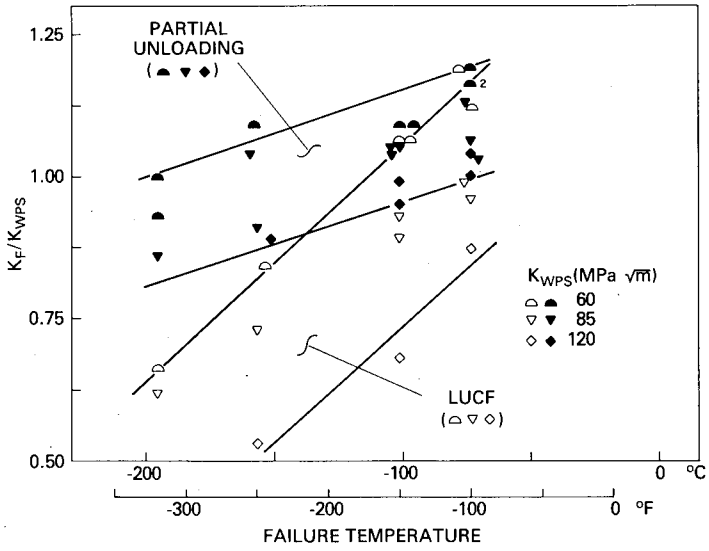

Fig. 7 — Relationship between the failure level K_F for three-point bend specimens and (a) warm prestress level K_{WPS}, (b) failure temperature, and (c) degree of unloading. The term LUCF is defined in Fig. 2.

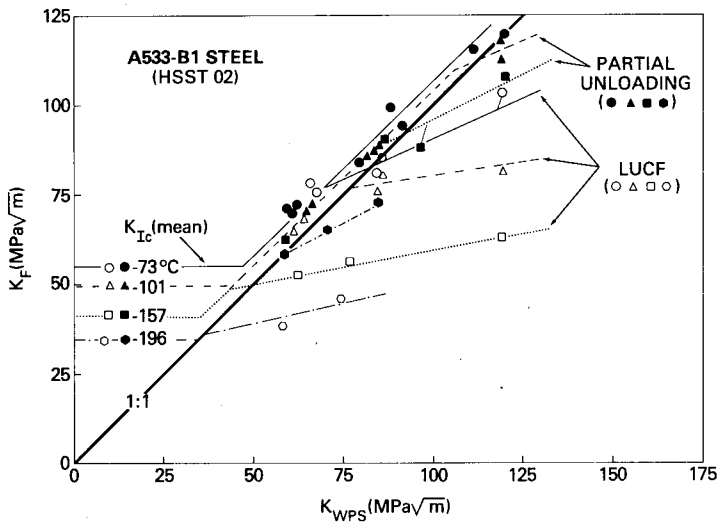

Fig. 8 — Comparison of the fracture level K_F and the warm prestress level K_{WPS}. The mean K_{Ic} values are taken from Fig. 3; the term LUCF is defined in Fig. 2.

Theoretical Model

A model depicting the interaction of reverse yielding and yield stress elevation is illustrated in Fig. 9 in terms of local stress vs local strain at the notch. A similar analysis has been discussed by Harrison and Fearnehough [1] and Andrews [3]. First, consider the case of a preload applied to 20°C, followed by either a partial or complete unloading such that reverse yielding at the crack tip does not occur as the load is reduced (ABCD in Fig. 9). During loading, local yielding "effectively" blunts the crack tip on a microscale. (BC). After unloading the temperature is decreased and the specimen is reloaded. The reloading will follow path DC (neglecting the slight increase in modulus at the lower temperature). This load must reach the preload level without the occurence of fracture; this is true whether or not the K_{Ic} of virgin material has been exceeded upon reloading.

The basis for the preceding conclusion is that the reloading occurs elastically. At C the specimen must exhibit a crack front shape and a stress distribution exactly as they were during the preloading at 20°C. Upon reloading, fracture will not occur at loads less than those corresponding to C because the crack tip blunting during the preloading (or, alternatively, the favorable residual stress pattern after unloading) precludes the local stress level from achieving the cleavage fracture stress σ_f. On the other hand, a separate, low temperature loading of a virgin specimen to the same *load* that resulted in stress C during the warm preloading would cause a *stress* level higher than C. A low temperature loading could proceed along path CL and thereby attain σ_f because of the stress intensification associated with the sharp crack. Therefore, for this example, it is concluded that fracture of the warm prestressed specimen can occur only upon a reload application that exceeds the original level, thereby resulting in an effective elevation in K_{Ic}.

Consider the next case of warm prestress applied at 20°C followed by complete or partial unloading such that reverse plastic flow occurs at the notch (ABEFG in Fig. 9). During the reverse yielding (FG) the blunted crack tip is effectively resharpened* by the compressive loading. Next the temperature is decreased and reloading proceeds along path GH. Because of the high stress intensity associated with the sharpened crack tip it is not possible to predict whether the preload level will be exceeded during reloading. However, it can be inferred that the probability of achieving the preload level again diminishes in proportion to the amount of reverse yielding. Consequently, it appears that the benefits of warm prestress vary inversely with the degree of unloading (i.e., reverse plastic flow).

On being reloaded the specimen will continue along path GH to point J because of the higher yield strength associated with the low temperature reloading; failure will occur when σ_f is reached (K). In this case one must be careful not to associate the local *stress* level H with a specimen *load* of a magnitude between the loads that resulted in stresses C and E during preloading. Because the crack tip is resharpened during unloading (FG), a local stress of magnitude H can be achieved at a lower load than was associated with a stress of magnitude H during preloading.

*The effective resharpening may be considered as a reduction of the crack-tip plastic zone and not as a geometric resharpening. In other words, the reversed yielding can wipe out the favorable residual stress pattern created by the plastic flow during loading.

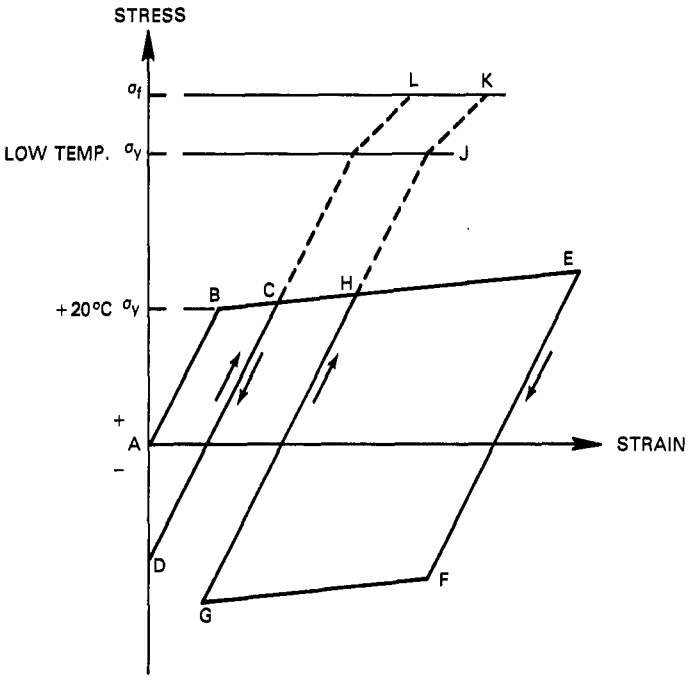

Fig. 9 — Behavior of local stress vs local strain at the crack tip during warm prestress

Finally, consider how the magnitude of ΔT might affect the fracture behavior upon reloading. For a small, or zero, ΔT one would always expect the preload to be attained upon reloading even with reverse plastic flow* (i.e., similar to fatigue cycling at a warm temperature). On the other hand, consider the stress-vs-strain behavior at H with a large ΔT. During the first loading, plastic flow was taking place at H. With reloading, the elastic behavior will continue beyond level H along path GJ until the fracture stress is reached (K). Furthermore, it is possible for the critical stress level σ_f to be reached at a load less than a preload. From this it is concluded that the benefit of warm prestress decreases in proportion to the magnitude of ΔT.

The above model appears to offer a satisfactory explanation for the experimental behavior observed in Fig. 8. For example, the warm prestress load was always achieved upon reloading for the case of small ΔT and partial unloading. This fact is attributed to the lack of reversed yielding. On the other hand, a partial or complete unloading and a large ΔT were associated with failures below the original warm prestress load. This fact is associated with a reverse plastic flow, notch sharpening, and attainment of σ_f upon reloading, as described by the model. Finally, one would expect the K_F deviations from the 1:1 line in Fig. 8 to be greater as K_{WPS} is increased. This can be explained by the greater amount of unloading (and greater reversed yielding) to which the specimens were subjected with the higher K_{WPS} levels.

*The possibility of strain again embrittlement by the reverse plastic flow has been considered. However, the short duration of the LOCA and the relatively low temperatures involved suggest that strain aging is an extremely remote possiblility [9].

Effect of Biaxial Loading

During a LOCA and operation of the emergency core cooling system, the thermal loading of the vessel causes a 1:1 biaxial stress state in the uncracked material. Consequently, positive stresses are created both normal to the crack plane and parallel to the crack front. In the present study it was assumed that biaxial loading of the vessel would not be a significant factor affecting the material response following *WPS*. In particular, these experiments have demonstrated that crack initiation will not occur as K_I decreases with time even if K_{Ic} is exceeded. This behavior reflects the generally accepted belief that increasing strain at the crack tip is a necessary condition for crack extension, excluding the case of corrosion cracking. During a LOCA the strain level exhibits a monotonic decrease with time following *WPS*. (The vessel is not repressurized.) This is the case whether or not biaxial loading is considered. Consequently, the presence of biaxial loading during the LOCA is not expected to alter the conclusion that, due to *WPS*, crack initiation will not occur at any time after which the *WPS* loading was effected.

STRUCTURAL INTERPRETATION OF *WPS* DURING A LOCA

A theoretical analysis of the potential for crack extension during a LOCA has been performed by Cheverton [4] for a typical pressurized water reactor vessel. This analysis is termed a reference calculational model (RCM). Cheverton's results are interpreted here to characterize the maximum depth of crack extension when considering the influence of *WPS*. The time-dependent stress intensities computed from Cheverton's analysis for a long, axial crack are presented in Figs. 10, 11, and 12. The following assumptions were made in modeling the vessel:

- Wall thickness = 216 mm (8.5 in.)
- Inner wall fluence = 4×10^{19} n/cm^2 E > 1 MeV (Corresponding to a 40-year irradiation period)
- High impurity copper level (> 0.25%, corresponding to severe radiation embrittlement)
- Preirradiation K_{Ic} vs temperature as defined by Westinghouse Corp. [5,6] for A533-B steel.
- Vessel not pressurized during the LOCA.

As previously described, decreasing fluence and increasing temperature toward the outside wall surface provide a mechanism for arresting a running crack that may initiate in the material of relatively low toughness near the inner wall surface. Arrest is assumed to occur when the K_{IR}* value exceeds the K_I value at the crack tip. Furthermore, the degradation in K_{IR} caused by neutron bombardment through the wall has been characterized in the subject analysis according to the procedures of Regulatory Guide 1.99 [10]. The guide defines the

*The K_{IR}-vs-relative-temperature behavior for reactor pressure vessel material is defined in Section III of the ASME Boiler and Pressure Vessel Code. The mechanics of crack arrest is a topic of current research; presently there is no guarantee that crack arrest will occur exactly when $K_I = K_{IR}$.

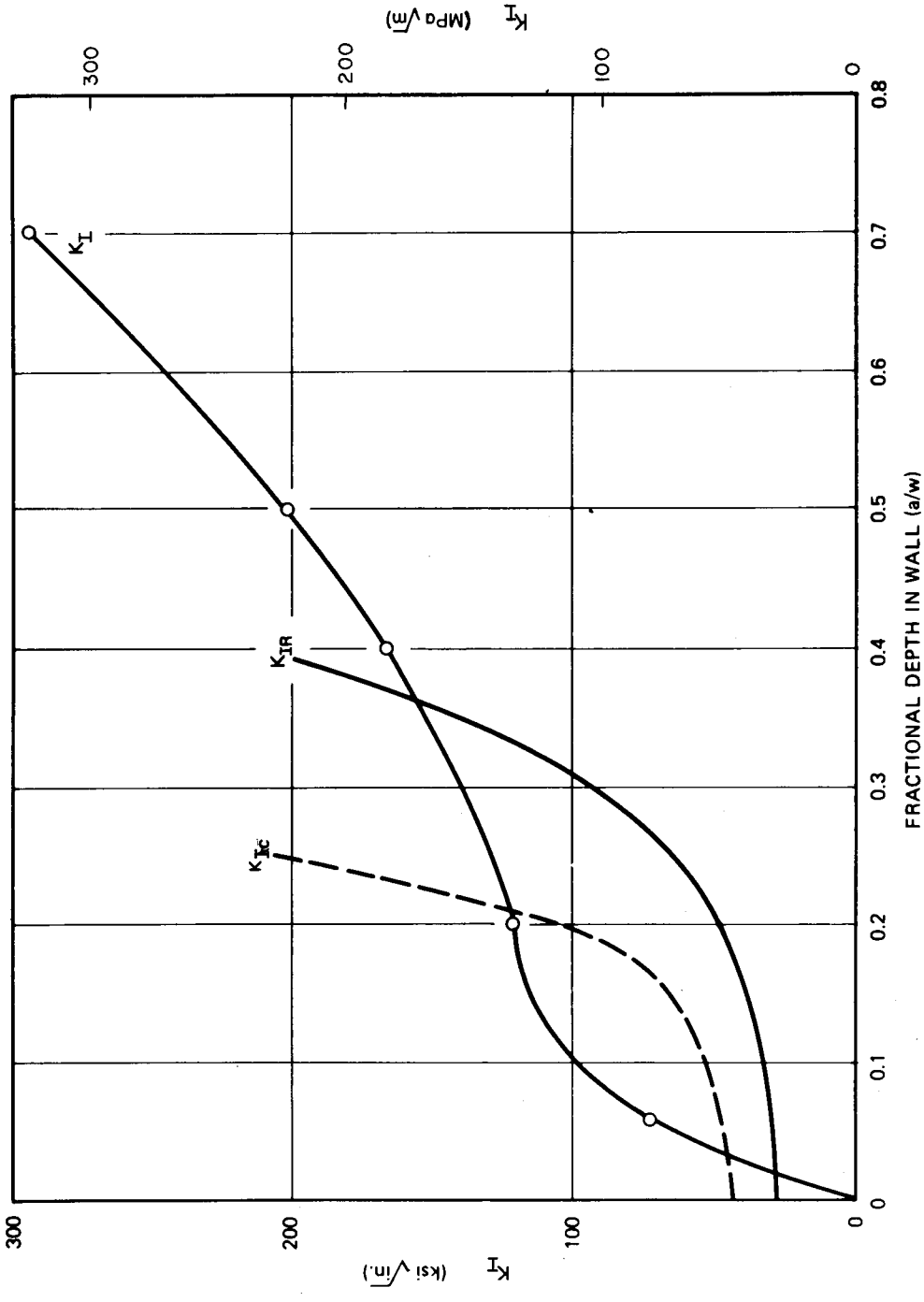

Fig. 10 — Illustration of the critical levels for initiation K_{Ic} and arrest K_{IR} as defined by the intersection of these curves with the K_I level for a long-axial flaw 7.5 min after the LOCA initiation [4]

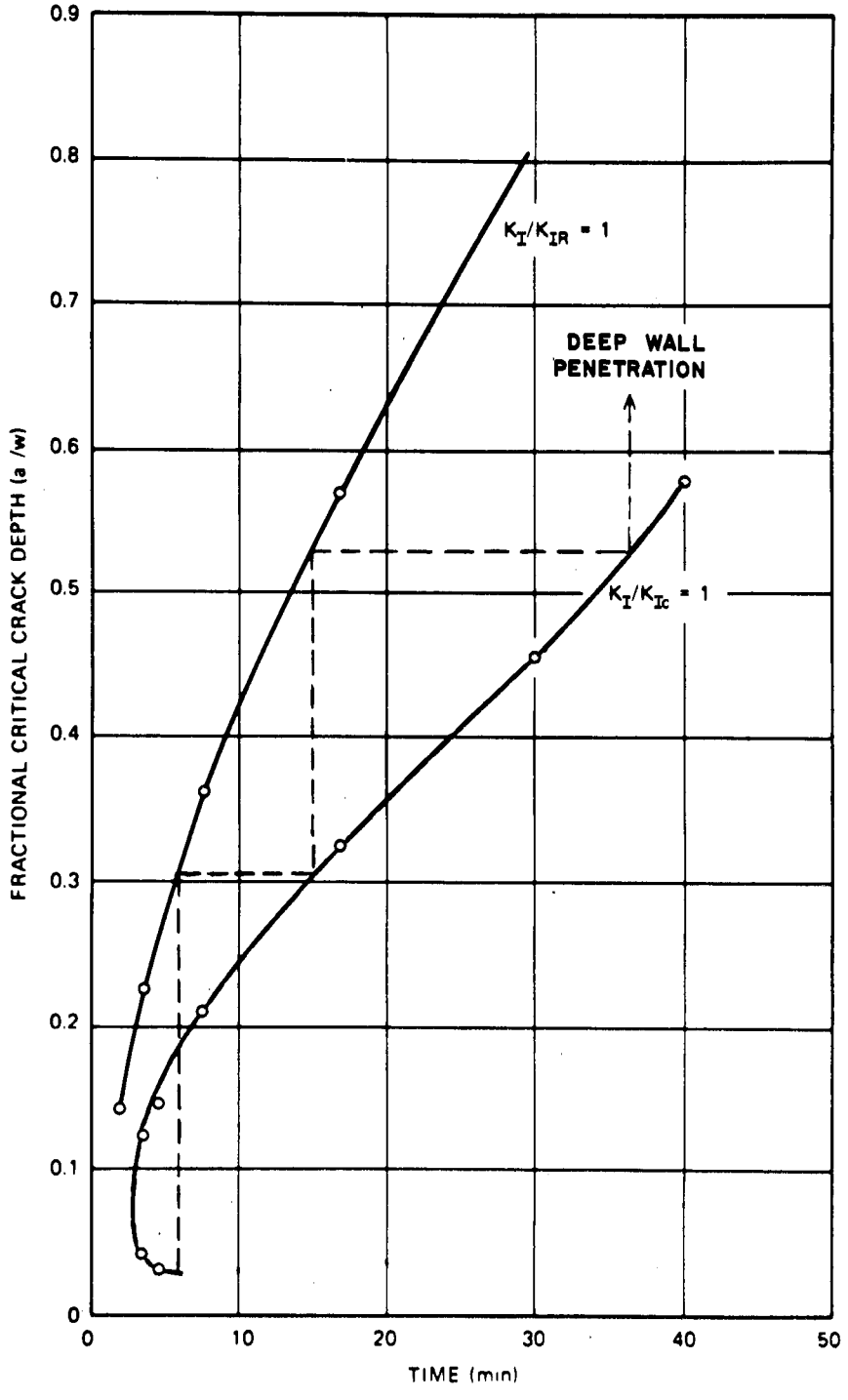

Fig. 11 — Crossplot of the intersections of K_I with K_{Ic} (e.g., Fig. 10) at various times [4]

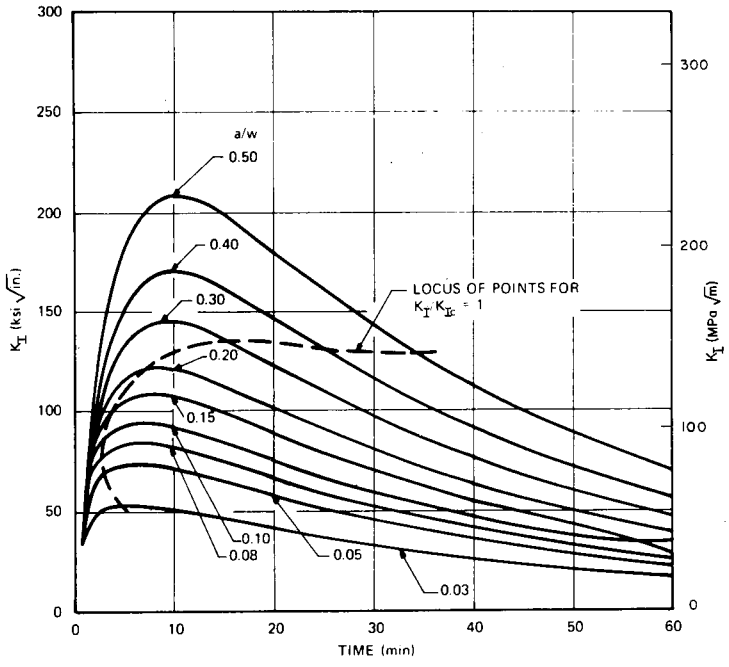

Fig. 12 — Stress intensity factor K_I vs time for different relative crack depths a/W, showing the locus of points at which the critical level for initiation K_{Ic} would be attained in the absence of warm prestress [4]

K_{IR}-vs-relative-temperature trend for irradiated material by a simple temperature translatic of the preirradiation trend, based on the fluence level and residual impurity content of the steel. In the reference calculational model the K_{Ic}-vs-temperature trend for the irradiated material has been obtained by the identical temperature translation.

Figure 10 illustrates the K_I level for a long axial flaw 7.5 min after the LOCA initiation. From the first intersection of K_I and K_{Ic} it is concluded that an axial crack having a depth-to-wall-thickness ratio (a/W) of 0.03 will initiate at this time. The flaw will propagat to a relative depth of $a/W = 0.36$ before it is assumed to arrest. Note that arrest occurs at a K_I level exceeding the value of K_{Ic} at the point of initiation. This is made possible becaus the crack extends into a region of increasing temperature which, in turn, provides significantly higher values of K_{IR} that act to arrest the crack. It should be noted that different size flaws can initiate at different times; Fig. 10 represents crack initiation conditions only at 7.5 min.

Figure 11 shows a cross plot of the intersections of K_I with K_{Ic} and K_{IR} at various times. The dashed line illustrates the progressive initiation, arrest, reinitiation behavior of a shallow crack. This description suggests that the crack could very nearly penetrate the wall. However, Cheverton [4] has pointed out that the assumptions of his model are conservative and that complete wall penetration may not actually take place. The K_I calculations were based on linear elastic behavior. For large crack penetrations ($a/W > 0.5$) the remaining ligament is subjected to plastic deformation and the assumption of linear elastic

behavior is not valid. The presence of plasticity will result in K_I levels less than those computed elastically and therefore will decrease the propensity to penetrate the wall [11].

Figure 12 depicts the behavior of K_I with time for a family of long, axial flaws. It is important to note both the relationship between these curves and the locus of points for which K_I/K_{Ic} is unity. With flaws of relative depth (a/W) greater than 0.2, the intersection of K_I and K_{Ic} occurs with decreasing K_I. This points out that all cracks greater than a relative depth of 0.2 have been warm prestressed. Nevertheless, on the basis of the NRL investigations, it is possible to predict crack extension to relative depths greater than 0.2. Consider a flaw of relative depth of 0.1 in the framework of Fig. 11. Since this flaw is not subject to *WPS*, it will begin to extend at a time of 3 min and will penetrate to a relative depth of 0.2. Because only cracks of relative depth greater than 0.2 are subject to *WPS*, the crack will reinitiate at a time of 7 min and extend to a relative depth of 0.34. Further extension is not likely at 18 min into the event when reinitiation would normally be predicted in the absence of *WPS*.

The preceding description illustrates that although crack initiation from shallow cracks cannot be prevented by *WPS*, the magnitude of the crack extension can be limited by this phenomenon so as to preclude complete penetration of the wall. The benefit of *WPS* is such that a potentially severe accident, that of complete wall penetration, is reduced to one of lesser severity in which the vessel integrity is maintained.

SUMMARY AND CONCLUSIONS

The present research investigations have considered the phenomenon of warm prestress and its potential benefit in minimizing crack extension during a LOCA. It is concluded that the mechanisms associated with *WPS* act to effectively elevate the critical fracture toughness K_{Ic} of the material at the crack tip. During a LOCA, the K_{Ic} is elevated when the peak value of *WPS*, K_{WPS}, is applied at a high enough temperature so that the K_{Ic} of the material exceeds K_{WPS}. After this peak loading to K_{WPS}, the K_I level in the vessel decreases and achieves the critical K_{Ic} value at a lower temperature (because of the temperature dependence of K_{Ic}). This study has demonstrated that failure never occurs during unloading. This observation is of major significance to the integrity of a prototype vessel. From this observation it is concluded that crack initiation will not take place in a vessel once the crack tip has been subjected to *WPS*. This conclusion is valid regardless of either the degree to which K_I at the crack tip falls below K_{Ic} or the nature of the unloading path. In other words, crack extension after *WPS* can take place only with increasing K_I; since K_I does not increase after the peak K_{WPS}, a necessary prerequisite for crack extension has been eliminated.

In terms of margin of safety against fracture, this study has shown that the effective elevation in K_{Ic} caused by *WPS* is not uniform. The elevation in K_{Ic} depends on (a) the *WPS* level, (b) the ΔT between the failure temperature and the temperature of *WPS*, and (c) the degree of unloading. The beneficial elevation of K_{Ic} appears to be greatest when both the ΔT and the degree of unloading are small. Fortunately, both conditions are met during a LOCA and an elevation of K_{Ic} should be assured by the *WPS* phenomenon. In particular, it is concluded that *WPS* can result in an elevation in K_{Ic} up to the *WPS* level during a LOCA transient, assuming of course, that metallurgically the material is capable of exhibiting

this level of toughness. Projections of the experimental data trends suggest that, with smaller ΔT values, the *WPS* phenomenon will elevate the K_{Ic} to the *WPS* level for even greater levels of *WPS* than those considered here (i.e., 120 MPa$\sqrt{\text{m}}$).

In these experiments, use of a relatively large ΔT was necessary to demonstrate unambiguously the effective elevation of K_{Ic} by *WPS*. During the LOCA, however, the ΔT can be much smaller than the values investigated. It is felt that a small ΔT will result in even greater benefit from *WPS* than was demonstrated by this study. To confirm this projection, experimental investigations are continuing at NRL to characterize the *WPS* phenomenon in the case of a small ΔT.

An interpretation of the structural significance of *WPS* has been made for a reference calculational vessel that was intended to consider the worst combination of conditions, including a long axial flaw and a wall that has suffered severe radiation embrittlement. Based upon an interpretation of K_I trends for this vessel computed by ORNL [4], it is concluded that *WPS* by itself cannot prevent the extension of shallow cracks. However, for the RCM containing a long-axial flaw, it is concluded that (a) a shallow crack ($a/W < 0.2$) can initiate and extend to a relative depth of 0.34 (further extension is precluded by *WPS*) and (b) a crack of initial relative depth greater than 0.2 is kept from extending by the *WPS* phenomenon.

Finally, it was observed that an elastic analysis of crack extension during a LOCA without *WPS* has predicted a deep penetration of the wall. The elastic analysis is conservative, and complete penetration of the wall may not actually occur. Nevertheless, the crack extension computed more exactly by means of a refined elastic-plastic model cannot be easily verified by full-scale experiments. The *WPS* phenomenon may eliminate the need for further elastic-plastic computations. More importantly, it may provide the key element upon which to predicate the integrity of the vessel during a LOCA.

ACKNOWLEDGMENTS

The authors express their appreciation to the U.S. Nuclear Regulatory Commission for its support of this research. Special thanks are due to E. K. Lynn (NRC) and G. R. Irwin (University of Maryland) for helpful discussions during this investigation.

REFERENCES

[1] T. C. Harrison and G. D. Fearnehough, "The Influence of Warm Prestressing on the Brittle Fracture of Structures Containing Sharp Defects," *Trans. ASME*, J. Basic Eng., 94 3-73 (June 1972).

[2] A. J. Brothers and S. Yukawa, "The Effect of Warm Prestressing on Notch Fracture Strength," *Trans. ASME*, J. Basic Eng., 85, 97 (Mar. 1963).

[3] W. R. Andrews, "Effect of Loading Sequence on Notch Strength of Warm Prestressed Alloy Steel," *Trans. ASME, J. Eng. Ind.* 92, 785-791 (Nov. 1970).

4. R. D. Cheverton, "Pressure Vessel Fracture Studies Pertaining to a PWR LOCA-ECC Thermal Shock: Experiments TSE-1 and TSE-2," ORNL/NUREG/TM-31, Oak Ridge National Laboratory, Sep. 1976.

5. W. O. Shabbits, "Dynamic Fracture Properties of Heavy Section A533-Grade B Class 1 Steel Plate," WCAP-7623, Westinghouse R & D Center, Pittsburgh, Pa., Dec. 1970.

6. W. O. Shabbits, W. H. Pryle, and E. T. Wessel, "Heavy Section Fracture Toughness Properties of A533 Grade B, Class 1 Steel Plate and Submerged Arc Weld Metal," WCAP-7414, Westinghouse R & D Center, Pittsburgh, Pa., Dec. 1969.

7. F. J. Loss, "Dynamic Tear Test Investigations of the Fracture Toughness of Thick-Section Steel," NRL Report 7056, May 14, 1970.

8. R. G. Berggren, "Heavy Section Steel Technology Program Semiannual Progress Report for Period Ending 28 February 1969," Oak Ridge National Laboratory, Oak Ridge, Tenn.

9. L. N. Succop, A. W. Pense, and R. D. Stout, "The Effects of Warm Overstressing on Pressure Vessel Steel Properties," *Welding J. Res. Suppl.* 49 354-s-364-s (Aug. 1970).

10. "Effects of Residual Elements on the Predicted Radiation Damage to Reactor Vessel Materials," Regulatory Guide 1.99, U.S. Nuclear Regulatory Commission, Office of Standards Development, Washington, D.C.

11. R. D. Cheverton, Personal communication, Oak Ridge National Laboratory, March 16, 1977.